

1 Title

2 Cross-reactive antibody responses against SARS-CoV-2 and seasonal common cold coronaviruses

3 Authors

4 Shelley Klompus^{1,2#}, Sigal Leviatan^{1,2#}, Thomas Vogl^{1,2##}, Iris N. Kalka^{1,2}, Anastasia Godneva^{1,2}, Eilat
5 Shinar³, Adina Weinberger^{1,2}, Eran Segal^{1,2*}

6

7 ¹Department of Computer Science and Applied Mathematics, Weizmann Institute of Science

8 ²Department of Molecular Cell Biology, Weizmann Institute of Science

9 ³Magen David Adom Blood Services, Israel

10

11 # Contributed equally

12 * Corresponding authors: thomas.vogl@weizmann.ac.il, eran.segal@weizmann.ac.il

13

14 ORCIDs

15 T.V.: 0000-0002-3892-1740

16

17 Abstract

18 Beyond SARS-CoV-2, six more coronaviruses infect humans (hCoVs), four of which cause only mild
19 symptoms (seasonal/common cold hCoVs) ^{1,2}. Previous exposures to seasonal hCoVs may elicit
20 immunological memory that could benefit the course of SARS-CoV-2 infections ³. While cross-reactive
21 T cells epitopes of SARS-CoV-2 and seasonal hCoVs have been reported in individuals unexposed to
22 SARS-CoV-2 ⁴⁻⁶, potential antibody-based cross-reactivity is incompletely understood.

23 Here, we have probed for high resolution antibody binding against all hCoVs represented as 1,539
24 peptides with a phage-displayed ⁷ antigen library. We detected broad serum antibody responses
25 against peptides of seasonal hCoVs in up to 75% of individuals. Recovered COVID-19 patients exhibited
26 distinct antibody repertoires targeting variable SARS-CoV-2 epitopes, and could be accurately
27 classified from unexposed individuals (AUC=0.96). Up to 50% of recovered patients also mounted
28 antibody responses against unique epitopes of seasonal hCoV-OC43, that were not detectable in
29 unexposed individuals.

30 These results indicate substantial interindividual variability and antibody cross-reactivity between
31 hCoVs from the direction of SARS-CoV-2 infections towards seasonal hCoVs. Our accurate high
32 throughput assay allows profiling preexisting antibody responses against seasonal hCoVs cost-
33 effectively and could inform on their protective nature against SARS-CoV-2.

34

NOTE: This preprint reports new research that has not been certified by peer review and should not be used to guide clinical practice.

35 Main text

36 COVID-19 (coronavirus disease 2019), caused by SARS-CoV-2 (severe acute respiratory syndrome
37 coronavirus 2), represents an unparalleled pandemic with millions of cases worldwide. In addition to
38 SARS-CoV-2, six more coronaviruses infect humans (hCoVs) including SARS-CoV-1 responsible for the
39 SARS outbreak in 2003 and MERS-CoV (Middle East respiratory syndrome) ¹. Four seasonal endemic
40 hCoVs (OC43, HKU1, NL63, 229E) are widely circulating in the population causing only mild symptoms
41 (common cold)². Previous exposures to seasonal hCoVs may elicit immunological memory that could
42 benefit the course of SARS-CoV-2 infections ³, which can range from asymptomatic to life-threatening
43 symptoms ⁸. The exact causes underlying this heterogeneity in COVID-19 severity are incompletely
44 understood and involve factors as age, gender, comorbidities, and preexisting immunity ^{9,10}. As an
45 important part of the adaptive immune system, it has been demonstrated that up to ca. 60% of
46 individuals unexposed to SARS-CoV-2 show CD4⁺ T cell recognition of its epitopes ^{4,5} and cross-
47 reactivity against seasonal hCoVs ⁶. Preexisting T cell or antibody responses need careful consideration
48 in vaccine development, with recommendations to assess existing immunity in vaccine trial
49 participants to ensure even distributions between testing groups ³.

50 Compared to studying T cell epitope recognition (which involves living cells, antigen presentation by
51 variable MHC alleles, and rather low affinity interactions ¹¹), antibody-antigen binding is robust, easily
52 detectable, and amenable to high throughput methods (e.g. ^{7,12}). Antibody tests for hCoV cross-
53 reactivity could be valuable tools to assess preexisting immunity at large-scale and stratify vaccine
54 trials cost effectively. Such serological testing could also inform on a possible impact of seasonal hCoVs
55 to herd immunity against SARS-CoV-2 ¹³. Yet, cross-reactive antibody responses between SARS-CoV-2,
56 seasonal hCoVs, and their protective potential are incompletely understood. It has been
57 demonstrated that antibodies of COVID-19 patients cross-react against full-length spike (S) and
58 nucleocapsid (N) proteins of SARS-CoV-1 and MERS-CoV ^{14,15}. However, there are differences in the
59 binding of protein segments, with antibodies binding the receptor-binding domain (RBD) of the SARS-
60 CoV-2 S-protein generally failing to bind this region of SARS-CoV-1 or MERS-CoV^{14,16,17}. Similarly, no
61 cross-reactivity between antibodies against the RBD of SARS-CoV-2 and seasonal hCoVs NL63/229E
62 was detectable ¹⁸. Epitope resolved antibody binding data beyond the S-protein/RBD is scarce for
63 SARS-CoV-2, and virtually unavailable for seasonal hCoVs ¹⁹.

64 Here, we have applied a high resolution antibody assay ^{7,12} to test for binding against 1,539 peptide
65 antigens covering all known proteins of all hCoVs. We have detected a high seroprevalence of seasonal
66 hCoVs in up to 75% of individuals both unexposed to SARS-CoV-2 and recovered from COVID-19,
67 variability in antibody repertoires against SARS-CoV-2, and cross-reactivity against seasonal hCoVs
68 upon SARS-CoV-2 infection.

69 Results and discussion

70 Antibody repertoires against hCoVs and cross-reactivities

71 Antibody binding against SARS-CoV-2 is typically assessed by ELISAs against full length
72 proteins/domains ^{20,21}, by resolving crystal structures ^{14,22}, or by peptide arrays ^{23,24}. Pinpointing
73 protein segments recognized by cross-reactive antibodies of all hCoVs requires high resolution and
74 high-throughput methods. Phage immunoprecipitation sequencing (PhIP-Seq) relies on the display of
75 synthetic oligo libraries on T7 phages ^{7,12}. Thereby displayed antigens can be rationally selected
76 allowing to probe for hundred thousands of antigens in parallel. After mixing of the phage library with
77 serum antibodies, unbound phages are washed away after immunoprecipitation and enriched phages
78 are detected by next generation sequencing (Fig. 1a).

79 We have generated a PhIP-Seq library covering all open reading frames of hCoVs as 64 amino acid (aa)
80 sections with 20 aa overlaps between adjacent peptides (Fig. 1b). The library also includes positive
81 controls which confirmed detection of antibody responses against viruses previously reported to elicit
82 population wide immunity¹² and negative controls, that did not show substantial binding (Table S 1).

83 We tested IgG antibody binding against this hCoV library with 32 serum samples of individuals
84 unexposed to SARS-CoV-2, that had been collected in 2013/2014²⁵ before the COVID-19 outbreak
85 (Fig. 1c). These antibody repertoires were compared to 32 samples of recovered COVID-19 patients
86 obtained in April and May 2020. In total we have assayed for nearly 100,000 antibody-peptide
87 interactions (1,539 hCoV peptides in each of the 64 individuals). Employing strict Bonferroni
88 correction, 240/1,539 peptides were enriched in at least one individual, with an average of 9 hCoV
89 peptides significantly bound per unexposed individual and 19 hCoV peptides in recovered COVID-19
90 patients. Most analyses were based on antibody responses against 57 hCoV peptides from 32 different
91 hCoV proteins, shared by more than five individuals of either group and seven peptides showing
92 significantly different abundances between the groups (Table S 2).

93 Unexposed individuals showed abundant antibody responses against all seasonal hCoVs: Binding
94 against peptides of hCoV-NL63 was detected in 75% of unexposed individuals, against hCoV-HKU1 in
95 66%, against hCoV-229E in 63%, and against hCoV-OC43 in 38% (Fig. 1h-k, Table S 2). The same
96 peptides were bound at similar frequencies in recovered COVID-19 patients and originated mostly
97 from S- or N-proteins (Table S 2). Binding of any peptide from seasonal hCoV S- or N- proteins was
98 detectable in 78% of unexposed individuals for hCoV-NL63, 75% for hCoV-HKU1, and 63% for hCoV-
99 229E and hCoV-OC43 with these epitope resolved results being in agreement with previous studies on
100 the seroprevalence of seasonal hCoVs using ELISAs²⁶.

101 Recovered COVID-19 patients' sera showed, as expected, an overrepresentation of several peptides
102 of SARS-CoV-2 that completely lacked binding in unexposed individuals, with five peptides passing FDR
103 (false discovery rate) correction for being significantly different between the two groups of individuals
104 (Table S 2). While nearly all COVID-19 patients showed binding against at least one peptide in S- or N-
105 proteins and some peptides being bound in up to 72% of recovered patients (Fig. 1e), no convergence
106 of antibody responses against the same peptide were detected in all individuals. This finding differs
107 from near universal recognition of some viral epitopes previously observed for other human viruses
108 (12) and replicated with controls in this study (S 1), suggesting that the antibody response against
109 SARS-CoV-2 can exhibit substantial inter-individual variability.

110 COVID-19 serum samples showed also common binding against SARS-CoV-1, indicating detection of
111 cross-reactivity of antibodies targeting SARS-CoV-2 (Fig. 1f) (14, 15), most notably one SARS-CoV-1
112 spike peptide had significantly enriched binding in up to 84% of COVID-19 recovered individuals
113 compared to 6% of unexposed individuals (Table S 2). A non-structural protein (NSP3) of SARS-CoV-1
114 was even bound in 13% of unexposed individuals and 22% of recovered, possibly owing to higher
115 conservation of such NSPs underlying less selective pressure than S- and N-proteins mostly responsible
116 for infectivity and targeted by neutralizing immune responses. A few other peptides were differentially
117 enriched between the two groups, but did not pass FDR correction for significance of this difference,
118 including a peptide of the MERS-CoV S-protein bound in 28% of COVID-19 sera and 3% (1/32) of
119 unexposed individuals (Fig. 1g).

120 Strikingly, cross-reactive responses from SARS-CoV-2 also extended to the seasonal hCoVs-OC43 (Fig.
121 1h). One hCoV-OC43 spike peptide was bound in 50% of COVID-19 sera and 3% (1/32) of unexposed
122 individuals, passing FDR correction for being differentially enriched between the two groups (Table S
123 2). Another two peptides of hCoV-OC43 spike were not bound in unexposed individuals at all, but
124 bound in up to 28% of COVID-19 patients, neither passing FDR correction (Table S 2). Differential

125 binding of hCoV-HKU1 was less pronounced with one peptide occurring in 19% of COVID 19 patients
126 and 3% (1/32) of unexposed individuals (Fig. 1i) not passing FDR correction (Table S 2). We did not
127 detect cross-reactivities against peptides from the alpha coronaviruses (hCoV-NL63 and CoV-229E),
128 with COVID-19 patients and healthy individuals' sera reacting at similar rates (Fig. 1j,k). Peptides
129 eliciting cross-reactive antibody responses between SARS-CoV-2, SARS-CoV-1, and seasonal hCoVs
130 typically originated from similar regions of S- (Fig. 2a) and N- (Fig. 2b) proteins. This data indicates that
131 epitopes in the SARS-CoV-2 spike S2 region are frequently bound in COVID-19 patients and a target
132 for cross-reactivity. Many recombinant SARS-CoV-2 vaccines in development focus either on the full-
133 length spike or the RBD alone²⁷. The observed S2 reactivity could lead to differences between these
134 designs, with responses against full-length S- protein vaccines potentially benefiting from cross-
135 reactivities against seasonal hCoVs, which may not occur for RBD only vaccines.
136 When looking at the principal components of an analysis (PCA, Fig. 3a) performed on the log fold
137 change (number of reads of bound peptides vs. baseline sequencing of phages not undergoing
138 immunoprecipitation) of significantly enriched oligos, unexposed individuals clustered together while
139 recovered COVID-19 patients' samples showed a greater spread. This illustrates the interindividual
140 variability in hCoV antibody responses elicited by SARS-CoV-2.

141 Overall, this data indicates that substantial cross-reactivity between hCoVs observed for T cells^{4,5} also
142 extends to antibody responses against seasonal hCoVs. We show that infection with SARS-CoV-2
143 mounts cross reactive antibodies against hCoV-OC43 antigens. The reverse direction of preexisting
144 antibody responses targeting seasonal hCoVs recognizing SARS-CoV-2 is more difficult to assess. We
145 observed binding of two SARS-CoV-2 epitopes in a few unexposed individuals (peptides from NSP2 in
146 19% and N protein in 6% (2/32), Table S 2). The abundance of responses against NSP2 did not change
147 in recovered COVID-19 patients, but binding of the N-protein antigen increased to 66% of recovered
148 patients. We also detected additional SARS-CoV-2 peptides bound in single healthy individuals
149 (including a spike peptide, Fig. 2a) similar to a population-wide abundance of 3% (1/32) in unexposed
150 individuals reported by a recent study comparing four antibody tests for the SARS-CoV-2 S/N proteins
151²⁸. hCoV peptides bound at higher abundance in unexposed individuals than recovered COVID-19
152 patients, would suggest a protective nature. As we did not detect any such peptides our data does not
153 support such a simple protective mechanism.

154 Assessing the protective nature of these population wide preexisting responses would require
155 comparing samples of the same individuals before and after contracting COVID-19 and information on
156 the course (severity) of the disease. The COVID-19 cohort of this study consisted of patients who had
157 experienced mild symptoms, and had not required hospitalization (testing positive in PCR and
158 serological tests). Employing our antigen library to compare antibody profiles against seasonal hCoVs
159 between mild and severe COVID-19 cases could also inform on protective effects of cross-reactivity,
160 as demonstrated for other aspects of the anti-SARS-CoV-2 immune response²⁹ and antibody binding
161 of SARS-CoV-2 proteins²⁰. If severe patients exhibited fewer antibody responses against antigens of
162 seasonal hCoVs, could point towards their protective nature. Moreover, possible detrimental effects
163 of cross-reactive antibody responses originating from seasonal hCoVs leading to antibody-dependent
164 enhancement³⁰ could be assessed with our hCoV antigen library.

165 hCov library based high throughput diagnostics

166 Testing for multiple hCoV antigens at high resolution in parallel could yield higher specificity than
167 conventional tests based on single proteins of SARS-CoV-2 by improving discrimination from seasonal
168 hCoVs. Most current SARS-CoV-2 serological tests rely on detection of entire S-/RBD or N-proteins,
169 reporting an aggregate of binding against all epitopes within^{21,31}. Interpreting the epitope-resolved
170 antibody binding data reported by our assay extends beyond conventional serological tests, as binding

171 against various epitopes of all hCoV needs to be weighed. We used machine learning to build a
172 predictor that highly accurately separated COVID-19 patients from healthy controls based on antibody
173 signatures (AUC=0.96, Fig. 3b). Depending on the intended application and cutoffs employed (Fig. 3c),
174 this assay can display 100% specificity at 72% sensitivity (reporting virtually no false-positives) or 94%
175 specificity at 91% sensitivity. Hence, in addition to informing on cross-reactivity between hCoVs, our
176 antigen library could also represent a tool for SARS-CoV-2 diagnostics.

177 From a technical perspective, our study shares general limitations of PhIP-Seq, most notable length
178 constraints of presented peptides (64 aa in this study) by underlying oligo synthesis and lack of
179 eukaryotic post translational modifications such as glycosylation. Opposed to neutralization assays
180 carried out with live viruses and cell cultures³¹, our data does not inform on the neutralizing capacity
181 of the observed binding events. While linear epitopes should be adequately covered, discontinuous,
182 conformational epitopes relying on the correct folding of domains could be missed. We did not
183 frequently detect binding to peptides of the RBD (with one adjacent peptide bound in 25% of COVID-
184 19 and 0% of unexposed individuals' sera, Fig. 2a), although other work and diagnostic tests relying
185 on the full length RBD had reported common antibody responses in COVID-19 patients^{14,16,17,21}. This
186 discrepancy may be due antibody responses against conformational epitopes in the RBD and/or a lack
187 of S protein glycans³³ in the phage displayed peptides.

188 While current oligo lengths employed in PhIP-Seq may underestimate conformational epitopes, it
189 provides a unique layer of information unobtainable from working with full length antigens or isolated
190 domains: Given the high resolution of the peptide approach, we pinpoint the exact bound regions
191 revealing crucial targets of cross-reactivities. Our hCoV antigen library can be leveraged to study
192 extended cohorts of patients with mild/severe disease courses or samples collected pre/post COVID-
193 19 infection, and could thereby inform on the potential protective nature of preexisting antibody
194 responses against seasonal hCoVs. In addition, our approach can be extended to other antibody
195 isotypes such as IgA, the primary mucosal antibody. Given the low cost of processing phage displayed
196 libraries in parallel³⁴, high accuracy (Fig. 3b,c), and its excellent amenability for robot automation^{12,34},
197 serological testing based on this hCoV library could be a broadly applicable tool to assess preexisting
198 immunity at population-scale (with implications towards protection and herd immunity of SARS-CoV-
199 2) as well as stratifying vaccine trial costs effectively.

200 Acknowledgments

201 E.S.'s COVID-19 research is supported by the Seerave Foundation. T.V. is supported by an Erwin
202 Schrödinger fellowship (J 4256) from the Austrian Science Fund (FWF).

203 Competing interests

204 The authors declare no competing interests.

205

206 Materials and methods

207 Samples

208 Serum samples of recovered COVID-19 patients were obtained from MDA (Magen David Adom, the
209 Israeli Red Cross equivalent). These samples had been collected from non-severe cases, who had not
210 been hospitalized. Before sampling, patients had tested twice negative by RT-qPCR testing.
211 Seropositivity of these samples had been confirmed by MDA with a commercial antibody test (Abbot,
212 SARS-CoV-2 IgG, ref. 6R86-22/6R86-32). Control serum samples of unexposed individuals had been
213 collected in 2013/2014 in Israel and reported in a previous study²⁵. Research with the COVID-19 serum
214 samples has been approved by the Weizmann Institute of Science's institutional review board (#1030-
215 4), and by the Tel Aviv Sourasky Medical Center for the samples of unexposed individuals (#0658-12-
216 TLV). Our cohorts of unexposed individuals and COVID-19 patients showed a different sex distribution
217 and minor age differences (Fig. 1c). While age/sex may influence COVID-19 serology of severe cases
218^{9,10,38,39}, we do not expect these parameters to affect key conclusions of our study in mildly affected
219 patients (with both cohorts also showing similar antibody responses against viral controls Table S 1b).

220 hCoV antigen library design

221 Reference genomes of the seven hCoVs were downloaded from NCBI directly using amino acid
222 sequences of the translated ORFs with the follow RefSeq accession numbers: SARS-CoV-2 -
223 NC_045512.2, SARS-CoV-1 - NC_004718.3, MERS-CoV - NC_019843.3, hCoV-OC43 - NC_006213.1,
224 hCoV-229E - NC_002645.1, hCoV-HKU1 - NC_006577.2, and hCoV-NL63 - NC_005831.2

225 For each strain the nonstructural proteins (NSPs) part of the large polyprotein 1ab (polyprotein 1a was
226 discarded if annotated) were separated. The SARS-CoV-2 polyprotein 1ab was cut according to the
227 table published by Wu *et al.*¹. Additional strains' polyproteins were processed by the following steps:
228 NSPs 1-3 were cut by sequences reported in the literature⁴⁰. The remaining NSPs, which are naturally
229 cut by 3Cl-like protease (3CLpro), were cut by the conserved protease cleavage site (small)-X-
230 (L/I/V/F/M)-Q#(S/A/G), where X is any amino acid and # represents the cleavage position⁴¹, and
231 multiply sequence alignment as verification of the site. Specifically for SARS-CoV-2, four additional
232 ORFs reported in the literature¹ (but not annotated in RefSeq NC_045512.2) were added.

233 The final list of proteins were cut to peptides of 64 amino acids (aa) with 20 aa overlaps (to cover all
234 possible epitopes of the maximal length of linear epitope⁴²) between adjacent peptides. The peptide
235 aa sequences were reverse translated to DNA using the *Escherichia coli* codon usage (of highly
236 expressed proteins), aiming to preserve the original codon usage frequencies, excluding restriction
237 sites for cloning (*EcoRI* and *HindIII*) within the coding sequence (CDS). The coding was re-performed,
238 if needed, so that a barcode was formed in the CDS, by the 44 nt at the 3' end of each oligo. Every
239 such barcode is a unique sequence at Hamming distance three from all prior sequences in the library,
240 which allows for correcting of a single read error in sequencing the barcode. For similar peptide
241 sequences, alternative codons were used following *E. coli* codon usage, to achieve discrimination.
242 Including the sequencing barcode as part of the CDS, rather than a separate barcode, allowed to use
243 the entire oligo for encoding a peptide (and as opposed to completely omitting a barcode, it did not
244 require sequencing the complete CDS). After finalizing the peptide sequence, the *EcoRI* and *HindIII*
245 restriction sites, stop codon, and annealing sequences for library amplification were added and
246 obtained from Agilent Technologies as 230mer pool (library amplification primers, fwd:
247 GGACCGCGACTGGAATTCT, rev: CCCGGGCATGAAGCTTTCA) and cloned into T7 phages following the
248 manufacturers recommendations (Merck, T7Select®10-3 Cloning Kit, product number 70550-3).

249 In this process we had also included controls of viral proteins with high population wide
250 seroprevalence previously reported¹² [11 proteins covered by 199 peptides] and negative controls of

251 42 random peptides and a human protein (SAP4K, 27 peptides) not expected to elicit binding in
252 healthy individuals. A full list of peptides included within the library as well as the corresponding amino
253 acid and nucleotide sequences is provided in supporting file S 3.

254 Phage immunoprecipitation sequencing

255 The PhIP-Seq experiments were performed as outlined in a published protocol ⁷ with the following
256 modifications: PCR plates for the transfer of beads and washing were blocked with 150 μ L BSA (30 g/L
257 in DPBS buffer, incubation overnight at 4°C) and BSA was added to diluted phage/buffer mixtures for
258 immunoprecipitations (IPs) to 2 g/L. We reasoned that the Generalized Poisson (GP) distribution
259 approach ⁴³ for calling bound peptides may be biased by frequent binding within this hCoV library,
260 leading to a skewed non-binding baseline for estimating GP parameters. Hence, we mixed the hCoV
261 library with a library of 244,000 microbiota and viral antigens that had previously shown a reliable
262 detectability and ratio of bound/unbound peptides (manuscript in preparation). Three microgram of
263 serum IgG antibodies (measured by ELISA) were mixed with the phage library (4,000-fold coverage of
264 phages per library variant). As technical replicates of the same sample were in excellent agreement,
265 measurements were performed in single reactions.

266 The phage library and antibody mixtures were incubated in 96 deep well plates at 4°C with overhead
267 mixing on a rotator. Forty microliters of a 1:1 mixture of protein A and G magnetic beads (Thermo
268 Fisher Scientific, catalog numbers 10008D and 10009D, washed according to the manufacturers
269 recommendations) were added after overnight incubation and incubated on a rotator for at 4°C. After
270 four hours, the beads were transferred to PCR plates and washed twice as previously reported ⁷ using
271 a Tecan Freedom Evo liquid handling robot with filter tips. The following PCR amplifications for pooled
272 Illumina amplicon sequencing were performed with Q5 polymerase (New England Biolabs, catalog
273 number M0493L) according to the manufacturers recommendations (primer pairs PCR1:
274 tcgtcggcagcgtcagatgtgtataagagacagGTTACTCGAGTGCGGCCGCAAGC and
275 gtctcgtgggctcggagatgtgtataagagacagATGCTCGGGGATCCGAATTC, PCR2: Illumina Nextera
276 combinatorial dual index primers, PCR3 [of PCR2 pools]: AATGATACGGCGACCACCGA and
277 CAAGCAGAAGACGGCATAACGA ⁷). PCR3 products were cut from agarose gel and purified twice (1x
278 QIAquick Gel Extraction Kit, 1x QIAquick PCR purification kit; Qiagen catalog numbers 28704/28104)
279 and sequenced on an Illumina NextSeq machine (custom primers for R1: ttactcagtgctggccgcaagctttca,
280 and for R2: tgtgtataagagacagatgtctcggggatccgaattct, R1/R2 44/31 nts). Paired end reads were
281 processed as described below.

282 Data analysis

283 Enriched peptides were calculated (after down-sampling to 1.25 million IDable reads per sample, i.e.
284 reads with a barcode within one error of the set of possible barcodes of the two mixed libraries for
285 which the paired end matched the IDed oligo) by comparing reads of input coverage (library
286 sequencing of phages before IPs) following a Generalized Poisson distribution approach, parameters
287 for which were estimated for each sample separately, as previously reported ⁴³. Derived p-values were
288 subject to Bonferroni correction (p-value 0.05) for multiple hypothesis testing, and log-fold-change
289 (number of reads of bound peptides vs. baseline sequencing of phages not undergoing IPs) was
290 computed for all peptides which passed the threshold p-value, all other peptides were given a log-
291 fold-change value of 0.

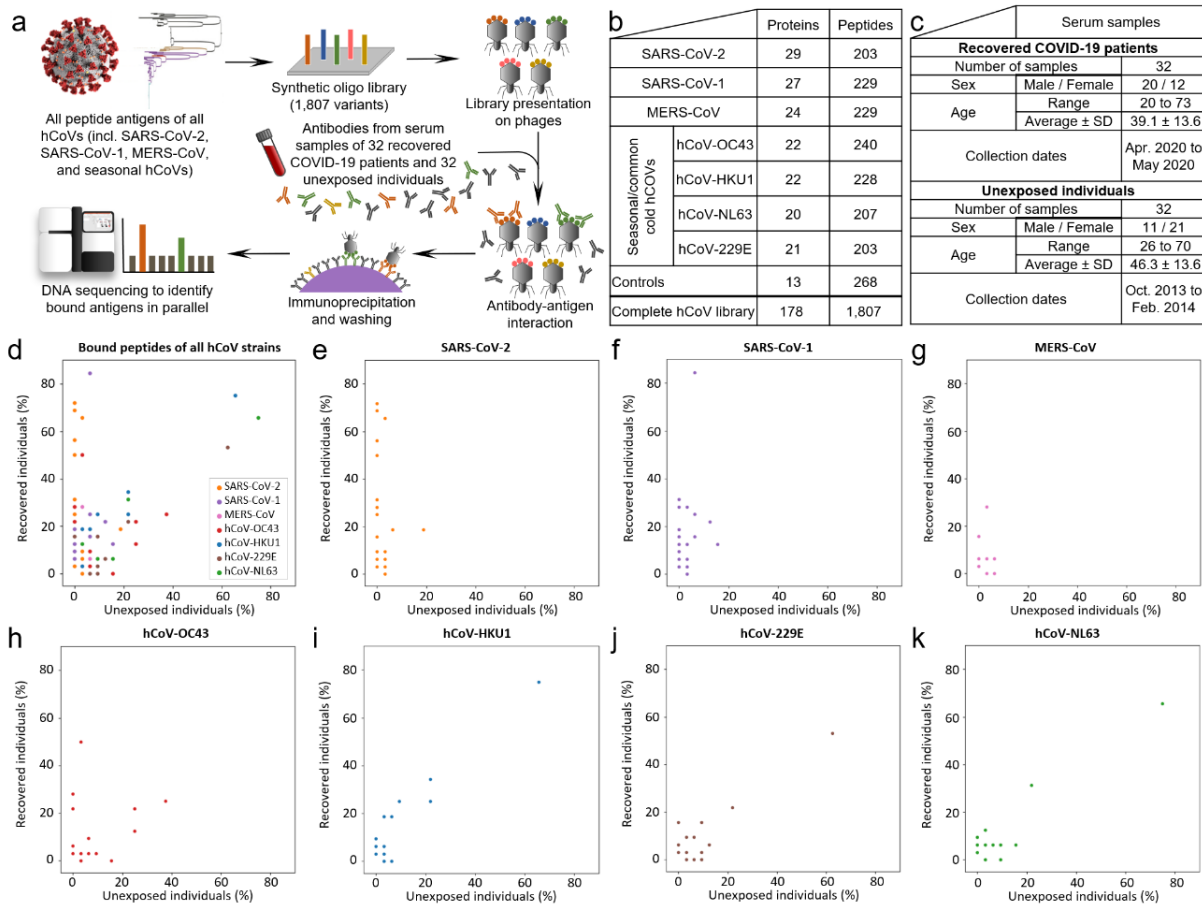
292 All oligo creation code, and analysis code was written in Python, using the libraries scikit-learn ⁴⁴, scipy,
293 statsmodels, pandas, numpy and matplotlib.

294 Alignments shown in Fig. 2 were created with CLC Main Workbench 6 (default settings).

295

296 Figures

297 Fig. 1



298

299 **Fig. 1: A phage displayed antigen library (a) of human Coronaviruses' peptide antigens (b) applied**
 300 **to serum samples of unexposed individuals and recovered COVID-19 patients (c) detects a high**
 301 **serum prevalence of seasonal hCoVs, interindividual variability of antibody repertoires against**
 302 **SARS-CoV-2, and cross-reactive antibody responses from SARS-CoV-2 infection (d-k).** The numbers
 303 of proteins per strain in panel b include polyproteins being split into 14 separate proteins. d-k, All
 304 bound antigens of the hCoV library are shown in panel d, the following panels depict binding against
 305 peptides of each hCoV strain separately. The illustration of the SARS-CoV-2 virion is reproduced from
 306 CDC PHIL #23312 released as public domain (CDC/ Alissa Eckert, MSMI; Dan Higgins, MAMS), the
 307 phylogenetic tree is reproduced from Wu et al. ¹ [open access].

308

309 Fig. 2

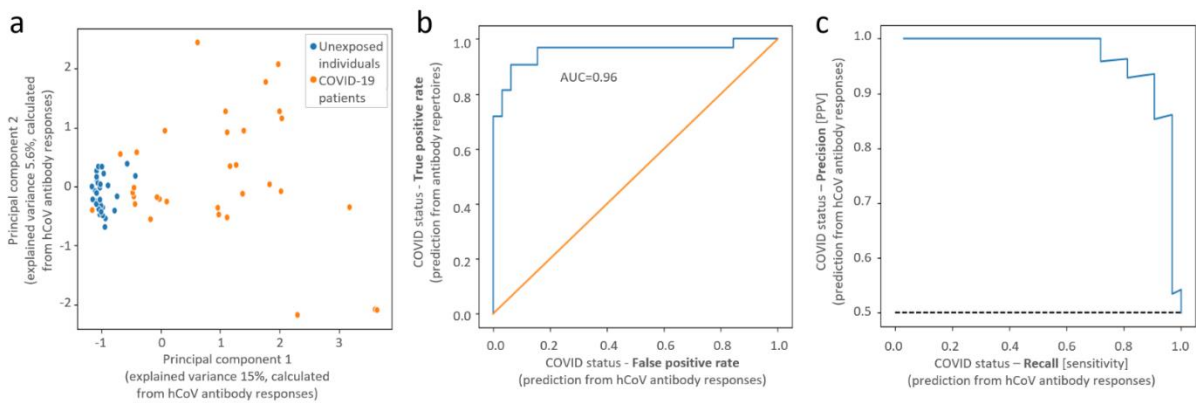


310

311 **Fig. 2: Cross-reactive and selective antibody binding of SARS-CoV-2 peptides and other hCoVs**
 312 **clusters in similar regions of the spike (a) and nucleocapsid (b) protein.** Alignments of S- and N-
 313 proteins of all hCoVs, the dark line next to the strain identifier represents the protein sequence
 314 indicating gaps in the consensus alignment. Peptides bound in more than five unexposed ('U')
 315 individuals or recovered COVID-19 patients ('C') are shown as arrows above the corresponding protein
 316 sequence. The abundance of binding in 'U' and 'C' is indicated as percentages written next to the
 317 peptides. Grey arrows indicate similar recognition in unexposed individuals and COVID-19 patients,
 318 blue arrows indicate more than two-fold overrepresented binding in COVID-19 patients. Peptides
 319 marked with an asterisk appear at significantly different abundances (passing FDR correction)
 320 between unexposed individuals and recovered COVID-19 patients, by scoring the difference between
 321 the two distributions of the log fold changes (number of reads of bound peptides vs. baseline
 322 sequencing of phages not undergoing IPs) of the two groups (Table S 2). The domain structure on top
 323 of each panel is based on SARS-CoV-2 S-³⁵/N-³⁶ proteins, positions in other hCoVs shift along the
 324 alignment. Due to the different lengths of S- and N- proteins, the two panels are not drawn at the
 325 same scale.

326

327 Fig. 3



328

329 **Fig. 3:** Principal component analysis (PCA) separates between hCoV antibody responses of
330 unexposed individuals and recovered COVID-19 patients (a) and a machine learning predictor
331 accurately identifies infected individuals (b,c). Gradient boosting decision trees (XGBoost classifier³⁷)
332 with leave-one-out cross-validation were used for these predictions on hCoV peptides bound in >4
333 (5%) individuals. Area under the curve (b) and precision-recall curve (c) of predicting COVID-19 status
334 from antibody responses against hCoV peptides (abbreviations: PPV - positive predictive value).

335

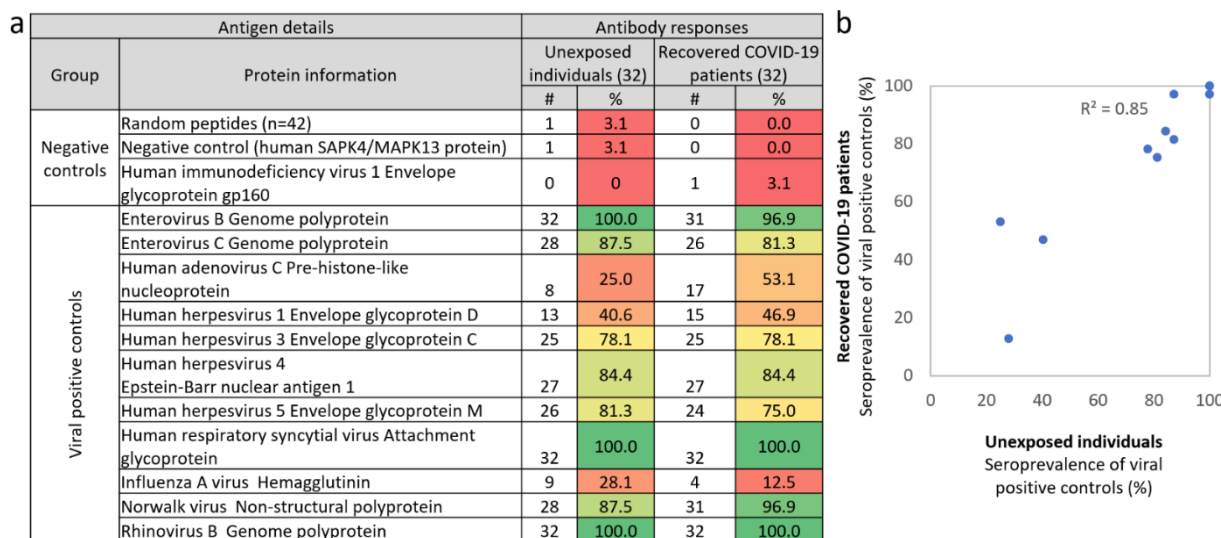
336 References

- 337 1. Wu, A. *et al.* Genome Composition and Divergence of the Novel Coronavirus (2019-nCoV)
338 Originating in China. *Cell Host Microbe* **27**, 325–328 (2020).
- 339 2. Walls, A. C. *et al.* Structure, Function, and Antigenicity of the SARS-CoV-2 Spike Glycoprotein.
340 *Cell* 1–12 (2020). doi:10.1016/j.cell.2020.02.058
- 341 3. Sette, A. & Crotty, S. Pre-existing immunity to SARS-CoV-2: the knowns and unknowns. *Nat.*
342 *Rev. Immunol.* (2020). doi:10.1038/s41577-020-0389-z
- 343 4. Grifoni, A. *et al.* Targets of T Cell Responses to SARS-CoV-2 Coronavirus in Humans with
344 COVID-19 Disease and Unexposed Individuals. *Cell* **181**, 1489-1501.e15 (2020).
- 345 5. Le Bert, N. *et al.* SARS-CoV-2-specific T cell immunity in cases of COVID-19 and SARS, and
346 uninfected controls. *Nature* (2020). doi:10.1038/s41586-020-2550-z
- 347 6. Mateus, J. *et al.* Selective and cross-reactive SARS-CoV-2 T cell epitopes in unexposed
348 humans. *Science (80-.)*. **21**, eabd3871 (2020).
- 349 7. Mohan, D. *et al.* PhIP-Seq characterization of serum antibodies using oligonucleotide-
350 encoded peptidomes. *Nat. Protoc.* **13**, 1958–1978 (2018).
- 351 8. Vabret, N. *et al.* Immunology of COVID-19: current state of the science. *Immunity* (2020).
352 doi:10.1016/j.immuni.2020.05.002
- 353 9. Scully, E. P., Haverfield, J., Ursin, R. L., Tannenbaum, C. & Klein, S. L. Considering how
354 biological sex impacts immune responses and COVID-19 outcomes. *Nat. Rev. Immunol.* **20**,
355 442–447 (2020).
- 356 10. Márquez, E. J., Trowbridge, J., Kuchel, G. A., Banchereau, J. & Ucar, D. The lethal sex gap:
357 COVID-19. *Immun. Ageing* **17**, 1–8 (2020).
- 358 11. Woodsworth, D. J., Castellarin, M. & Holt, R. A. Sequence analysis of T-cell repertoires in
359 health and disease. *Genome Med.* **5**, 98 (2013).
- 360 12. Xu, G. J. *et al.* Viral immunology. Comprehensive serological profiling of human populations
361 using a synthetic human virome. *Science* **348**, aaa0698 (2015).
- 362 13. Kissler, S. M., Tedijanto, C., Goldstein, E., Grad, Y. H. & Lipsitch, M. Projecting the
363 transmission dynamics of SARS-CoV-2 through the postpandemic period. *Science (80-.)*. **182**,
364 eabb5793 (2020).
- 365 14. Ju, B. *et al.* Human neutralizing antibodies elicited by SARS-CoV-2 infection. *Nature* **584**,
366 (2020).
- 367 15. Wec, A. Z. *et al.* Broad neutralization of SARS-related viruses by human monoclonal
368 antibodies. *Science (80-.)*. **736**, eabc7424 (2020).
- 369 16. Premkumar, L. *et al.* The receptor binding domain of the viral spike protein is an
370 immunodominant and highly specific target of antibodies in SARS-CoV-2 patients. *Sci.*
371 *Immunol.* **5**, 1–10 (2020).
- 372 17. Yuan, M. *et al.* A highly conserved cryptic epitope in the receptor-binding domains of SARS-
373 CoV-2 and SARS-CoV. *Science* **7269**, 2020.03.13.991570 (2020).
- 374 18. Amanat, F. *et al.* A serological assay to detect SARS-CoV-2 seroconversion in humans.
375 *medRxiv* 2020.03.17.20037713 (2020). doi:10.1101/2020.03.17.20037713
- 376 19. Kellam, P. & Barclay, W. The dynamics of humoral immune responses following SARS-CoV-2
377 infection and the potential for reinfection. *J. Gen. Virol.* (2020). doi:10.1099/jgv.0.001439
- 378 20. Atyeo, C. *et al.* Distinct Early Serological Signatures Track with SARS-CoV-2 Survival. *Immunity*
379 1–9 (2020). doi:10.1016/j.immuni.2020.07.020
- 380 21. Weissleder, R., Lee, H., Ko, J. & Pittet, M. J. COVID-19 diagnostics in context. *Sci. Transl. Med.*
381 **12**, 1–6 (2020).
- 382 22. Barnes, C. O. *et al.* Structures of human antibodies bound to SARS-CoV-2 spike reveal
383 common epitopes and recurrent features of antibodies. *Cell* 1–15 (2020).
384 doi:10.1016/j.cell.2020.06.025

- 385 23. Jiang, H. wei *et al.* SARS-CoV-2 proteome microarray for global profiling of COVID-19 specific
386 IgG and IgM responses. *Nat. Commun.* **11**, 1–11 (2020).
- 387 24. Li et al., Linear epitope landscape of SARS-CoV-2 Spike protein constructed from 1,051
388 COVID-19 patients, (2020), *medRxiv* doi:10.1101/2020.07.13.20152587
- 389 25. Zeevi, D. *et al.* Personalized Nutrition by Prediction of Glycemic Responses. *Cell* **163**, 1079–94
390 (2015).
- 391 26. Gorse, G. J., Patel, G. B., Vitale, J. N. & O’Connor, T. Z. Prevalence of antibodies to four human
392 coronaviruses is lower in nasal secretions than in serum. *Clin. Vaccine Immunol.* **17**, 1875–
393 1880 (2010).
- 394 27. World Health Organization, Draft landscape of COVID-19 candidate vaccines – 13 August
395 2020, [https://www.who.int/publications/m/item/draft-landscape-of-covid-19-candidate-](https://www.who.int/publications/m/item/draft-landscape-of-covid-19-candidate-vaccines)
396 [vaccines](https://www.who.int/publications/m/item/draft-landscape-of-covid-19-candidate-vaccines)
- 397 28. Grzelak, L. *et al.* A comparison of four serological assays for detecting anti-SARS-CoV-2
398 antibodies in human serum samples from different populations. *Sci. Transl. Med.* **3103**, 1–18
399 (2020).
- 400 29. Arunachalam, P. S. *et al.* Systems biological assessment of immunity to mild versus severe
401 COVID-19 infection in humans. *Science* **6261**, 1–18 (2020).
- 402 30. Arvin, A. M. *et al.* A perspective on potential antibody-dependent enhancement of SARS-CoV-
403 2. *Nature* **8**, 1–11 (2020).
- 404 31. Krammer, F. & Simon, V. Serology assays to manage COVID-19. *Science (80-.).* **368**, 1060–
405 1061 (2020).
- 406 32. Whitman, J. D. *et al.* Evaluation of SARS-CoV-2 serology assays reveals a range of test
407 performance. *Nat. Biotechnol.* (2020). doi:10.1038/s41587-020-0659-0
- 408 33. Watanabe, Y., Allen, J. D., Wrapp, D., McLellan, J. S. & Crispin, M. Site-specific glycan analysis
409 of the SARS-CoV-2 spike. **9983**, 1–9 (2020).
- 410 34. Larman, H. B. *et al.* PhIP-Seq characterization of autoantibodies from patients with multiple
411 sclerosis, type 1 diabetes and rheumatoid arthritis. *J. Autoimmun.* **43**, 1–9 (2013).
- 412 35. Wrapp, D. *et al.* Cryo-EM structure of the 2019-nCoV spike in the prefusion conformation.
413 *Science* **367**, 1260–1263 (2020).
- 414 36. Cubuk *et al.* (2020) The SARS-CoV-2 nucleocapsid protein is dynamic, disordered, and phase
415 separates with RNA, preprint, *bioRxiv* doi:10.1101/2020.06.17.158121
- 416 37. Chen, T. & Guestrin, C. XGBoost: A Scalable Tree Boosting System. in *Proceedings of the 22nd*
417 *ACM SIGKDD International Conference on Knowledge Discovery and Data Mining* 785–794
418 (ACM, 2016). doi:10.1145/2939672.2939785
- 419 38. Takahashi, T. *et al.* Sex differences in immune responses that underlie COVID-19 disease
420 outcomes. *Nature* (2020). doi:10.1038/s41586-020-2700-3
- 421 39. Bunders, M. & Altfeld, M. Implications of sex differences in immunity for SARS-CoV-2
422 pathogenesis and design of therapeutic interventions. *Immunity* **2**, 1–9 (2020).
- 423 40. Yang, X. *et al.* Proteolytic processing, deubiquitinase and interferon antagonist activities of
424 Middle East respiratory syndrome coronavirus papain-like protease. *J. Gen. Virol.* **95**, 614–626
425 (2014).
- 426 41. Snijder, E. J., Decroly, E. & Ziebuhr, J. The Nonstructural Proteins Directing Coronavirus RNA
427 Synthesis and Processing. *Adv. Virus Res.* **96**, 59–126 (2016).
- 428 42. Forsström, B. *et al.* Dissecting antibodies with regards to linear and conformational epitopes.
429 *PLoS One* **10**, 1–11 (2015).
- 430 43. Larman, H. B. *et al.* Autoantigen discovery with a synthetic human peptidome. *Nat.*
431 *Biotechnol.* **29**, 535–41 (2011).
- 432 44. Buitinck *et al.* API design for machine learning software: experiences from the scikit-learn,
433 (2013) ECML PKDD Workshop: Languages for Data Mining and Machine Learning 108-122
434

435 Supporting information

436 S 1



437

438 **S 1: Control antigens included in the library demonstrate low background signal of unspecific binding**
 439 **against random peptides and reproducible antibody recognition of previously reported viral**
 440 **antigens¹² with similar abundances between unexposed individuals and recovered COVID-19**
 441 **patients (b).** Peptide negative controls within the hCoV antigen library included 42 random peptides,
 442 peptides of the human protein SAPK4 (which should not elicit autoreactive antibodies in healthy
 443 individuals), and an HIV protein (with HIV infection being an exclusion criterion for participation in this
 444 study). Only 1/42 random peptides and one peptide of the human protein SAPK4 were bound in a
 445 single individual, indicating a low background of unspecific binding (or cross-reactivity). Yet, this result
 446 indicates that peptides appearing at low signal strengths in single individuals may arise from
 447 nonspecific binding. To eliminate such peptides, the following analyses of viral antigens (with
 448 population wide seroprevalence previously reported¹²) was performed using a cut-off of at least two
 449 peptides appearing per virus per individual (or peptides occurring in at least four individuals) to count
 450 as positive. Following analyses of hCoV binding and predictions were performed with these or even
 451 more stringent cutoffs.

452 Serum prevalence for non-hCoV viral antigens were similar between unexposed individuals and
 453 recovered COVID-19 patients (b). The slight differences of seroprevalence in unexposed individuals
 454 and recovered COVID-19 patients for Human adenovirus C and Influenza A virus antigens may be due
 455 the cohort sizes or age/gender differences.
 456

457 S 2

458 **S2: Most frequent hCoV antigens bound in unexposed individuals and recovered COVID-19 patients.**

459 Abundance of antibody responses against peptides of hCoV proteins detected in more than four
460 individuals of either cohort are listed. Multiple peptides originating from the same protein are
461 summarized. The seven peptides indicated by bold text are significantly different between unexposed
462 individuals and recovered COVID-19 patients, by scoring the difference between the two distributions
463 of the log fold changes (number of reads of bound peptides vs. baseline sequencing of phages not
464 undergoing IPs) of the two groups. Peptides passing FDR are marked with an '*' and peptides passing
465 also Bonferroni correction with a '#'.
466

| Antigen details | | | | Antibody responses | | | |
|--|--|---------------------|-----------------------------------|----------------------------|------|----------------------------------|------|
| Strain | Protein | Protein length (aa) | Starting position of peptide (aa) | Unexposed individuals (32) | | Recovered COVID-19 patients (32) | |
| | | | | Number of individuals | % | Number of individuals | % |
| SARS-CoV-2 | Nucleocapsid phosphoprotein (YP_009724397.2) | 419 | 133 | 2 | 6.3 | 6 | 18.8 |
| | | | 353*# | 0 | 0.0 | 23 | 71.9 |
| | | | 356*# | 0 | 0.0 | 22 | 68.8 |
| | | | 221 | 0 | 0.0 | 9 | 28.1 |
| | | | 89 | 0 | 0.0 | 5 | 15.6 |
| | Spike (Surface glycoprotein, YP_009724390.1) | 1273 | 793*# | 1 | 3.1 | 21 | 65.6 |
| | | | 1145*# | 0 | 0.0 | 18 | 56.3 |
| | | | 1101*# | 0 | 0.0 | 16 | 50.0 |
| | | | 749 | 0 | 0.0 | 10 | 31.3 |
| | 529 | 0 | 0.0 | 8 | 25.0 | | |
| Membrane glycoprotein (YP_009724393.1) | 222 | 159 | 1 | 3.1 | 3 | 9.4 | |
| NSP2 (YP_009724389.1) | 638 | 89 | 6 | 18.8 | 6 | 18.8 | |
| SARS-CoV-1 | Nucleocapsid protein (NP_828858.1) | 422 | 359 | 0 | 0.0 | 9 | 28.1 |
| | | | 353 | 1 | 3.1 | 9 | 28.1 |
| | | | 133 | 2 | 6.3 | 8 | 25.0 |
| | | | 177 | 0 | 0.0 | 6 | 18.8 |
| | | | 89 | 0 | 0.0 | 5 | 15.6 |
| | | | 221 | 1 | 3.1 | 4 | 12.5 |
| | Spike (E2 glycoprotein precursor, NP_828851.1) | 1255 | 793 | 2 | 6.3 | 27 | 84.4 |
| | | | 749 | 0 | 0.0 | 10 | 31.3 |
| | Matrix protein (NP_828855.1) | 221 | 158 | 0 | 0.0 | 4 | 12.5 |
| | NSP2 (NP_828849.2) | 638 | 89 | 5 | 15.6 | 4 | 12.5 |
| NSP3 (NP_828849.2) | 1922 | 925 | 4 | 12.5 | 7 | 21.9 | |
| | | 353 | 2 | 6.3 | 5 | 15.6 | |
| hCoV-MERS | Nucleoprotein (YP_009047211.1) | 413 | 350 | 0 | 0.0 | 5 | 15.6 |
| | | | 45 | 2 | 6.3 | 2 | 6.3 |
| | Spike glycoprotein (YP_009047204.1) | 1353 | 1189 | 1 | 3.1 | 9 | 28.1 |
| hCoV-OC43 | Nucleocapsid protein (YP_009555245.1) | 448 | 221 | 8 | 25.0 | 7 | 21.9 |
| | | | 1 | 3 | 9.4 | 1 | 3.1 |
| | | | 385 | 8 | 25.0 | 4 | 12.5 |
| | | | 353 | 5 | 15.6 | 0 | 0.0 |
| | Spike surface glycoprotein (YP_009555241.1) | 1353 | 1189*# | 1 | 3.1 | 16 | 50.0 |
| | | | 1233 | 0 | 0.0 | 9 | 28.1 |
| | | | 881 | 0 | 0.0 | 7 | 21.9 |
| | | | 617 | 2 | 6.3 | 3 | 9.4 |
| 749 | 12 | 37.5 | 8 | 25.0 | | | |

| Antigen details | | | | Antibody responses | | | |
|-------------------------------------|---|---------------------|-----------------------------------|----------------------------|------|----------------------------------|------|
| Strain | Protein | Protein length (aa) | Starting position of peptide (aa) | Unexposed individuals (32) | | Recovered COVID-19 patients (32) | |
| | | | | Number of individuals | % | Number of individuals | % |
| hCoV-HKU1 | Nucleocapsid phosphoprotein (YP_173242.1) | 441 | 221 | 3 | 9.4 | 8 | 25.0 |
| | Spike glycoprotein (YP_173238.1) | 1356 | 1233 | 1 | 3.1 | 6 | 18.8 |
| | | | 881 | 2 | 6.3 | 6 | 18.8 |
| | | | 617 | 21 | 65.6 | 24 | 75.0 |
| | | | 749 | 7 | 21.9 | 8 | 25.0 |
| Membrane glycoprotein (YP_173241.1) | 223 | 1 | 7 | 21.9 | 11 | 34.4 | |
| hCoV-229E | Nucleocapsid protein (NP_073556.1) | 389 | 326 | 0 | 0.0 | 5 | 15.6 |
| | | | 45 | 7 | 21.9 | 7 | 21.9 |
| | | | 1 | 3 | 9.4 | 1 | 3.1 |
| | Surface glycoprotein (NP_073551.1) | 1173 | 661 | 0 | 0.0 | 5 | 15.6 |
| | | | 441 | 20 | 62.5 | 17 | 53.1 |
| | NSP2 (NP_073549.1) | 786 | 529 | 3 | 9.4 | 5 | 15.6 |
| | | | 485 | 2 | 6.3 | 3 | 9.4 |
| NSP12 (NP_073549.1) | 927 | 397 | 4 | 12.5 | 2 | 6.3 | |
| NSP13 (NP_073549.1) | 597 | 441 | 1 | 3.1 | 3 | 9.4 | |
| hCoV-NL63 | Nucleocapsid protein (YP_003771.1) | 377 | 177 | 7 | 21.9 | 10 | 31.3 |
| | | | 314 | 2 | 6.3 | 2 | 6.3 |
| | | | 265 | 3 | 9.4 | 2 | 6.3 |
| | | | 45 | 24 | 75.0 | 21 | 65.6 |
| | NSP2 (YP_003766.2) | 788 | 397 | 1 | 3.1 | 4 | 12.5 |
| NSP12 (YP_003766.2) | 927 | 397 | 5 | 15.6 | 2 | 6.3 | |

466

467 S 3

468 **S 3: Supporting xlsx file with a full list of peptides included within the library as well as the**
469 **corresponding amino acid and nucleotide sequences (including controls).** For each displayed peptide
470 the organism of origin and protein name (including the accession number in the relevant databases
471 NCBI/UniProt/GISAID) is provided. Starting positions of the peptides in the protein's sequence are
472 provided. Twenty-nine peptides were identical between multiple hCoVs (indicated by the last column
473 'Identical to peptide #') and are highlighted in bold.